

Twist glass transition in regioregulated poly(3-alkylthiophene)s

Koji Yazawa and Yoshio Inoue

Department of Biomolecular Engineering, Tokyo Institute of Technology. 4259 Nagatsuta-cho,
Midori-ku, Yokohama, Kanagawa 226-8501, Japan

Takakazu Yamamoto

Chemical Resources Laboratory, Tokyo Institute of Technology. 4259 Nagatsuta-cho,
Midori-ku, Yokohama, Kanagawa 226-8503, Japan

Naoki Asakawa

Department of Biomolecular Engineering, Tokyo Institute of Technology. 4259 B-55 Nagatsuta-cho,
Midori-ku, Yokohama, Kanagawa 226-8501, Japan

(Dated: April 15, 2024)

The molecular structure and dynamics of regioregulated poly(3-butylthiophene) (P3BT), poly(3-hexylthiophene) (P3HT), and poly(3-dodecylthiophene) (P3DDT) were investigated using Fourier transform infrared absorption (FTIR), solid state ^{13}C nuclear magnetic resonance (NMR), and differential scanning calorimetry (DSC) measurements. In the DSC measurements, the endothermic peak was obtained around 340 K in P3BT, and assigned to enthalpy relaxation that originated from the glass transition of the thiophene ring twist in crystalline phase from results of FTIR, ^{13}C cross-polarization and magic-angle spinning (CPMAS) NMR, ^{13}C spin-lattice relaxation time measurements, and centerband-only detection of exchange (CODEX) measurements. We defined this transition as twist-glass transition, which is analogous to the plastic crystal - glassy crystal transition.

I. INTRODUCTION

Poly(3-alkylthiophenes) (P3ATs) show great promise as electronic and optoelectronic devices such as light-emitting diodes and field-effect transistors. Particularly, the regioregular versions of P3ATs have received much attention because they show high crystallinity and high conductivity because of improvement of main chain packing.

Their structures have been studied extensively to gain understanding of the physical properties of P3ATs. In particular, polymorphic behavior among three solid phases has been a main topic in structural investigation^{1,2,3,4,5}: Phase I, mainly taking an end-to-end arrangement for side chains; Phase II, molecular packing with interdigitation, in which the side chains are intercalated; and the nematic mesophase. The realization of the phases depends strongly on the alkyl side chain length and their thermal histories. Although it is said that the P3ATs with longer alkyl chains are likely to form Phase II, correlation between the side chain length and the resultant phase has never been clearly determined.

The dynamic structure of P3AT is important to find out physical properties such as thermochromism, in which the twist motion of the thiophene ring is thermally excited⁶. Conformation is an elemental excitation related to such molecular structural defects that it behaves as an interrupter of π -conjugation. Therefore, the dynamics as well as dimension and density of conformations are related closely to the conjugation length of the electron^{7,8}. No studies are available for the molecular dynamics of P3ATs in spite of its importance.

Phases with conformation are called quasi-ordered

phases⁹. Typical examples of the quasi-ordered phase include liquid crystals (LCs) and plastic crystals (PCs). Generically, LCs are found in rod-type molecules having translational freedom, whereas PCs are realized in spherical molecules such as C_{60} , having translational symmetry, but rotational freedom. Particular attention has been devoted to the glass transitions of LCs^{10,11,12,13,14,15,16} and PCs^{17,18,19,20,21} to obtain information about the dynamics of quasi-ordered phases. Interestingly, some quasi-ordered phases can be frozen into a state called glassy liquid crystal (GLC) and glassy crystal (GC) if LCs and PCs are cooled rapidly enough. Investigating these phases helps us determine the dynamics of translational or rotational orders. They can serve as model systems for dynamics of the glass transition of amorphous polymer. Dynamics of quasi-ordered phases in polymers, however, have not been investigated and little is known on whether the glassy states produced from the quasi-ordered phases exist or not.

In this study, we shall give attention to the dynamics of quasi-ordered phases, particularly twist motion of thiophene main chain in the crystalline state of P3ATs. At first, we show an endothermic peak for poly(3-butylthiophene) (P3BT) in DSC measurements, and peak shifts of C-H out-of-plane deformation region in FTIR measurement around 340 K. Next, we also investigate the dynamics of P3BT around the transition by ^{13}C CPMAS NMR, ^{13}C spin-lattice relaxation time measurements ($T_{1\rho}$), and centerband-only detection of exchange (CODEX) measurements, and show evidence of the glass transition with respect to the twist motion. We define this transition as twist glass transition, which is an example analogous to PC-GC transition.

II. EXPERIMENTS

A. Materials

Regioregular HT (head-to-tail)-type poly(3-butylthiophene) (P3BT), poly(3-hexylthiophene) (P3HT), and poly(3-dodecylthiophene) (P3DDT) were purchased from Rieke Metals Inc.²² and were used without further purification.

B. DSC Measurements

The DSC thermograms of the powder P3ATs were recorded mainly on a differential scanning calorimeter (Pyris Diamond; PerkinElmer Inc.). Rapid quenching using liquid nitrogen and the second heating scan were performed on another calorimeter (Seiko DSC 220; Seiko Corp.). The respective masses of all samples were 3(6 mg. The temperature and heat flow scales were carefully calibrated at different heating rates using an indium standard with nitrogen purging.

C. FTIR Measurements

The FTIR measurements were carried out using an FTIR microscope (AIM-8800; Shimadzu Corp.) that was equipped with an FTIR hotstage (LK-600; Linkam Scientific Instruments, Ltd.) and a cooling unit (L600A). All spectra were recorded at a resolution of 2 cm⁻¹ and with an accumulation of 16 scans. Samples cast on BaF₂ substrates from the chloroform solution and dried in an oven under vacuum for 12 h were heated and cooled at a constant rate of 10 K/m in using nitrogen purging.

D. Solid-state NMR Measurements

We carried out variable temperature ¹³C cross-polarization and magic-angle spinning (CPMAS)²³, T₁ ρ , and centerband-only detection of exchange (CODEX)²⁴ measurements using a NMR spectrometer (GSX-270; JEOL) operating at 270 MHz for ¹H and 67.9 MHz for ¹³C. For CPMAS measurements, experimental conditions were set up with 90° pulse length of 5.2 μ s, contact time of 2 ms, recycle delay of 10 s, and the MAS rate of 3.2 kHz. The ¹³C chemical shifts were referenced externally to the methyl carbon resonance of hexamethylbenzene at 17.36 ppm. We used Torchia method²⁵ for T₁ ρ measurements. For CODEX measurements, experimental conditions were set up with 90° pulse length of 5.0 μ s, contact time of 2 ms, recycle delay of 10 s, and the MAS rate was monitored by fiber optics and set at 5000 \pm 2 Hz. Pure-exchange CODEX spectra are obtained by measuring a reference spectrum with durations of t_m and t_z interchanged and subtracting the CODEX spectrum from it. Original powder samples were used. We

also carried out variable temperature proton transverse relaxation time (T_{2H}) measurements. The detailed experimental conditions are in Supplementary Information.

E. Chemical shielding calculation

The ¹³C chemical shielding tensors of a model compound for HT poly(3-alkylthiophene) were calculated using an ab initio self-consistent field (SCF) coupled Hartree-Fock method with gauge invariant atomic orbitals (SCF-GIAO)^{26,27}. The HT-trimeric(3-methylthiophene) was employed for all calculations. Structural optimization assuming s-trans conformation and SCF-GIAO shielding calculations were carried out using the 6-31G(d) basis set. All ab initio chemical shielding calculations were performed using a Gaussian 98 (Rev A7) program package²⁸ run on a Cray C916/12256 supercomputer at the Computer Center, Tokyo Institute of Technology.

III. RESULTS AND DISCUSSION

A. DSC Measurements

Figure 1 shows DSC thermograms of the P3ATs measured on heating at a rate of 10 K/m in. Endothermic peaks were visible near 545 K, 500 K, and 435 K for P3BT, P3HT and P3DDT, respectively. These transitions are attributed to the melting of crystalline to the isotropic phase⁹. For P3DDT, another endothermic peak was observed around 330 K, which is consistent with the previous DSC study⁹. It is attributed to the melting of ordered side chains. Interestingly, P3BT gave rise to another endothermic transition around 340 K. It is difficult to assign this transition to the melting of side chains because the butyl group is inferred to be in a liquid-like state at that temperature because P3HT shows no similar peak over the range between 223 K and 500 K. Causin et al. reported similar DSC results and deduced from the results of wide angle x-ray diffraction (WAXD) of P3BT that the transition is a polymorphic behavior from the co-existing state between Phase II (interdigitation packing) and Phase I (end-to-end packing), to Phase I'. In the following, we will show evidence that the 340 K peak originates from a twist glass transition. Their study showed that the traces of diffraction conditions exhibited drastic changes between 323 K and 373 K. At 373 K, the (100) diffraction, attributed to side-by-side alignment, became sharper and more intense. The (010) signal ($d_{010} = 3.8$ Å), attributed to thiophene ring stacking, emerged from a very broad halo. On the other hand, the WAXD patterns of Phase II were not clear at 323 K; i.e. the (100) diffraction was weak and both Phase I and Phase II of (010) signals were not visible. Therefore, we inferred that no clear evidence exists to indicate polymorphism between Phase I and Phase II.

Chen et al. observed a similar endothermic peak at 332 K for regiorandom P3BT and attributed it to the glass transition temperature²⁹. However, they did not identify its type of glass transition. Figure 1 (b) and Fig. 1 (c) respectively show the second heating scans that were performed after the first heating scans and two versions of quenching procedures, with cooling at 50 K/m in and quenching by liquid nitrogen. We present a clear heat capacity jump that is believed to be a glass transition at 300 K in Fig. 1 (c). Figure 1 (b) shows no such jump, indicating that sufficiently rapid cooling prevents crystallization and gives rise to the conventional glass transition by cage effect³⁰. Therefore, we conclude that the both endothermic peaks at 332K which is observed by Chen et al. and at 340K by us are distinguishable from the conventional glass transition. Slight difference between two temperatures of Chen's and ours, 332K and 340K, are probably because of the difference of regioregularity. Since the regioregularity of our sample is higher than Chen's, the transition temperature would be higher due to the larger size of lamellar stacking.

B. Temperature Dependence of FTIR Spectra

We carried out *in situ* FTIR measurements on a thin film of P3BT to clarify the transition of P3BT around 340 K. Figure 2 shows FTIR absorption spectra of P3BT, P3HT, and P3DDT in the C-H out-of-plane deformation region as a function of temperature. First, we specially examine the behavior at temperatures greater than 303 K (right side of Fig. 2). For P3HT and P3DDT, single peaks were observed at 820 cm^{-1} at 303 K. A new band grew at 836 cm^{-1} , whereas the 820 cm^{-1} band decreased when both polymers were heated over the melting temperature of long range order of the main chain (Fig. 2 (b) and Fig. 2 (c)). This phenomenon was consistent with the previous FTIR study for regiorandom P3HT³¹. We can respectively assign two bands, 820 cm^{-1} and 836 cm^{-1} , to some sort of crystal and isotropic liquid.

Unlike those, P3BT showed somewhat complex spectral changes. Figure 3 shows temperature dependent absorbance at each wavenumber for P3BT. At 303 K, the strongest peak is at 825 cm^{-1} and a small shoulder is observed at 810 cm^{-1} . With heating, the intensity of the 820 cm^{-1} band grows while both 825 cm^{-1} and 810 cm^{-1} bands decrease. It is noteworthy that the temperature range at which spectral changes occur in the FTIR spectra are consistent with results of DSC measurement. From 353 K to 473 K, the band maximum remained at 820 cm^{-1} . Around melting temperature (540 K), the 820 cm^{-1} band disappeared, whereas the 836 cm^{-1} band grew, which resembles the melting behavior of P3HT and P3DDT. Therefore, the transition around 340 K must be a solid-solid transition because the melting temperature is much higher than 340 K. It differs, however, from a conventional glass transition mentioned by Cheng²⁹ because, below the transition temperature, P3BT shows an

x-ray diffraction peak at 7, which corresponds to the (100) plane because of the lamellar structure⁵. As mentioned above for the result of DSC, the second heating scan shows the heat capacity jump at 300 K, which is distinct from 340 K (Fig. 1 (c)).

We also carried out FTIR measurements below room temperature (303 K – 173 K) to elucidate the bands at 825 cm^{-1} and 810 cm^{-1} . The left side of Fig. 2 shows the temperature dependence of FTIR spectra for P3BT, P3HT, and P3DDT with cooling. Changes in the absorption of each peak (825 cm^{-1} , 820 cm^{-1} , and 810 cm^{-1}) for P3BT are shown in Fig. 3. In the lower temperature region, the absorbance at 825 cm^{-1} was approximately constant. However, the band at 820 cm^{-1} showed a gradual decrease. In addition, a small shoulder peak was apparent at 810 cm^{-1} . Changes between the two bands showed a clear isosbestic point: the component attributed to 820 cm^{-1} was converted directly to the component consisting of 810 cm^{-1} as the temperature decreased.

When heating from 173 K, we can respectively observe the increase and decrease of intensity of 825 cm^{-1} and 820 cm^{-1} bands from 310K to 360K. In DSC measurements (Fig. 1a), deviation from the baseline starts from 320K, and reaches peak top, which indicates the end of transition, at 340K. Since the temperature range of the transition observed in DSC and FTIR are consistent, both measurements must detect an identical transition.

In addition, P3HT also showed a gradual shift of the absorption maximum from 820 cm^{-1} to the lower wavenumber (815 cm^{-1}) with cooling. A higher wavenumber band than 820 cm^{-1} did not appear as P3BT, which shows a band of 825 cm^{-1} below 340 K. For P3DDT, a gradual shift from 820 cm^{-1} to a lower wavenumber was not observed, but slight glowing and peak narrowing at 805 cm^{-1} was observed. Among these polymers, only P3BT showed both a higher wavenumber shift around 340 K and a lower wavenumber shift between 340 K and 173 K with cooling.

A salient topic for the structure of P3ATs has been the polymeric behavior between Phase I and Phase II. However, it would be difficult to explain the IR measurement results using only two static phases for one reason. Although P3DDT is considered to show a transition from Phase II to Phase I around 330 K by the melting of alkyl chains^{1,2,5}, the maximum absorption was maintained at 820 cm^{-1} before and after the transition. The peak shift in P3BT reflects the reasons other than the polymeric phase.

C. ¹³C CPMASS NMR spectra, Spin-lattice Relaxation Time, and CODEX measurements

To investigate the structure and molecular dynamics of P3BT around 340 K, ¹³C CPMASS and ¹³C spin-lattice relaxation time measurements were performed for P3BT at various temperatures. The ¹³C CPMASS spectra of P3BT and the chemical shift of each carbon are shown

respectively in Fig. 4 and Table I. Chemical shifts of the alkyl chain are consistent with the gauche conformation of regiorandom poly(3-octylthiophene) (P3OT)⁴, indicating that the alkyl chains behave similarly to the liquid state.

It is noteworthy that the clear shoulder signal of the C4'(methyl) carbon of P3BT is apparent around 16.0 ppm below 333 K, whereas the spectra at the higher temperatures show a unique component (14.6 ppm), meaning that at least two chemically inequivalent methyl carbons in P3BT exist below 333 K. Because the methylene carbons show no peak splitting, only the end of the butyl chain shows two or more distinct states.

In Fig. 4(b), the signals of the thiophene ring for P3BT appear over the frequency region of 120{145 ppm as previous studies of oligothiophene³² and regiorandom poly(3-octylthiophene)⁴ have shown. We observed five peaks in all measured temperature ranges (Table I). On the other hand, Bolognesi et al.⁴ observed six peaks in the presence of both Phase I and Phase II for regiorandom poly(3-octylthiophene). They assigned the peaks at 140.2 ppm (C3) and 129.5 ppm (not assigned to any carbon) to Phase II because of agreement with the transition temperature observed by the x-ray diffraction. In our results, although a peak is apparent at 140.2 ppm, the peak at 129.5 ppm was not observed. Furthermore, although the intensity of the signal decreases with heating, the peak at 140.2 ppm exists at higher and lower temperatures than the transition temperature. This result is controversial to Causin's argument by the x-ray diffraction where Phase I only exist above the transition temperature. From these results, it is difficult to explain which peaks originate from Phase I or Phase II because two apparent differences between Bolognesi's and our samples are regioregularity and alkyl chain length. Therefore, this issue is still unclear. Consequently, we shall give attention only to four peaks, except for the peak at 140.2 ppm. Specifically regarding the line width, narrowing of C4 was observed with heating. To investigate the factors that cause this narrowing, we carried out T_{2H} measurement (see the Supplementary Information). The spin-spin relaxation rate (R_2) of a rigid moiety decreases with heating, although no sudden change was observed with respect to the transition around 340 K. Therefore, the motional narrowing of the local dipolar field occurs over the measuring temperature range. However, dynamic averaging of chemical shift distribution due to the twist motion possibly causes the narrowing of ^{13}C signal. The latter possibility cannot be ruled out only from the T_{2H} measurements. Conclusively, we could not identify the reason for the signal narrowing with respect to temperature elevation of the C4 carbon of thiophene. Broadening and Splitting of C2 and C5 with heating were also observed. We will discuss broadening later because it is expected to bear a relation with the spin-lattice relaxation time. The splitting may indicate the beginning of reorientational motion. We will also discuss the splitting later. Results of FTIR and CPMAS NMR show that the structural change of P3BT

occurs markedly around 340 K. At temperatures greater than 340 K, the state of the main chain is attributed almost uniquely to 820 cm^{-1} in FTIR. The side chain is also at a unique state, as shown by results of CPMAS NMR. Below 340 K, the main chain consists of mainly two states: the main component attributed to 825 cm^{-1} and the other to 810 cm^{-1} in FTIR spectra. The methyl moiety of the side chain also shows at least two components and is probably related to the main-chain states.

Two questions remain. What explains the absence of the (010) peak and the weakness of (100) peaks below 323 K in the WAXD measurement⁵? Even if both phases (Phase I and Phase II) coexist, the respective scattering peaks of x-ray diffraction should be observed. Furthermore, the peak shifts in the IR spectrum from 825 cm^{-1} and 810 cm^{-1} to 820 cm^{-1} with heating do not coincide with the argument by Causin et al.: the transition from Phase I and Phase II to Phase I because no common IR absorption peak attributable to Phase I is visible before and after the transition.

The other is the driving force of the transition. Clarifying the driving force would be the key to organizing the information obtained from FTIR, CPMAS NMR, and WAXD. Here, we specifically examine the dynamics of the twisting motion of the main chain in the crystalline state. Thermochromism phenomena for P3ATs are well known to result from the existence of quasi-ordered phase or mesophase: thiophene rings have sufficient degrees of freedom to allow a twisting motion. If the main chain had preserved the planarity without twisting until melting, we would not have observed gradual color changes. The slight melting heat flow bears out the existence of the mesophase. Additionally, the diffusion-like motion of the twisting was observed for a similar regioregular polymer, poly(4-methylthiazole-2,5-diyl) (P4MTZ), by solid-state NMR measurements³³.

We performed ^{13}C spin-lattice relaxation time measurements for P3ATs using Torchia method²⁵ at various temperatures to investigate the molecular dynamics. An Arrhenius plot of the spin-lattice relaxation rate ($R_1 = T_1^{-1}$) for each carbon is shown in Fig. 11.

For the side chains (Fig. 11(a)), each R_1 value was obtained using a simple exponential fitting curve:

$$M_z(t) = e^{-R_1 t}; \quad (1)$$

where M_z is the magnetization along the magnetic field. Figure 11(a) shows the subtle change of slopes around 333 K, but the decrease of R_1 was observed throughout the measured temperature range with heating (from 303 K to 373 K). This tendency is visible in the extremely narrowed regime according to the classical Bloembergen-Pound-Purcell (BPP) theory³⁴, indicating that the side chains behave similarly to liquid, which is also observed in ^{13}C CPMAS NMR spectra. The subtle change of slopes was inferred to result from the conformation change of the main chain because it would be difficult to believe that further changes in average conformation should occur in a liquid state. On the other hand, the re-

relaxation of main chain carbons showed no single exponential decay in the measured temperature range. For that reason, we tried to fit the decay curves using a Kohlrausch-Williams-Watts (KWW) function³⁵

$$M_z(t) / \exp\left(-\frac{t}{T_1}\right) : \quad (2)$$

In general, the KWW function is used to express magnetization near and below the glass transition temperature (T_g) because the distribution of the relaxation rate gave rise to non-exponential recoveries.³⁶ Temperature dependence of R_1 and stretching parameter extracted by Eq. (2) for each aromatic carbons are shown respectively in Figs. 11(b) and 6. Figure 11(b) shows that the main chain must be in the slow-motion regime because of the increase of R_1 with heating. More noteworthy is the fact that discontinuous changes are apparent around 333 K. In many cases, a similar tendency is apparent in ^2H NMR measurements, at the glass transition for many glassy formers³⁷ including polymers such as polybutadiene³⁸ and polystyrene³⁹. In the case of NMR spin-lattice relaxation measurements, we can distinguish three temperature regions for the arguments of glass transition. (i) $T < T_g$: The R_1 of glass formers is dominated by slow process (Johari-Goldstein process⁴⁰), which follows the Arrhenius-type thermal activation process below T_g . (ii) $T_g < T < 1.2T_g$: Both process and the Johari-Goldstein process affect R_1 . Where the process is described as stretched exponential functions. (iii) $T > 1.2T_g$: R_1 is dominated only by process.

Below 333 K, we observed the Arrhenius-type thermally activated process for all carbons. That tendency is similar to the Johari-Goldstein process. Over 333 K, although the measured temperature range is insufficient to consider the condition of (ii) or (iii) because of the limitation of available temperature range of our instrument, discontinuous changes can be a fingerprint for the effect of processes.

In Fig. 11(b), another remarkable point exists. For the CPMAS ^{13}C NMR measurements, relaxation occurs through two paths: that by fluctuation of a local field by ^{13}C - ^1H magnetic dipolar coupling and that by ^{13}C chemical shift anisotropy (CSA). Carbons that are directly connected to a proton, such as C4, have a larger dipolar coupling effect than that of unconnected carbons. Below 333 K, only the C4 carbon shows larger R_1 than other carbons, indicating that the relaxation is caused mainly by ^{13}C - ^1H magnetic dipolar coupling. That is, the thiophene ring does not undergo reorientations sufficient to fluctuate the chemical shift anisotropy. Over 333 K, the other carbons (C2, C3, C5) showed individually specific slopes, indicating that reorientation of the thiophene ring brings about fluctuation in CSA as well. The principal components of nuclear shielding for the modeling compound of HT-poly(3-methylthiophene) that are determined by GIAO-CHF also indicate the effects of CSA (Table II). The fact that the axis carbons (C2 and C5)

with the larger show steeper slopes over 333 K supports the effective CSA contribution. Furthermore, line broadening of C2 and C5 with increasing temperature, as mentioned above, is explainable by the steep increase of R_1 . That is, the well-known nonsecular broadening⁴¹.

There are two kinds of molecular motions that could affect CSA of thiophene carbons, translation and reorientation. However, the possibility of translational motion would be very small, because the diffraction peaks due to the π -stacking were observed in x-ray pattern above the transition temperature⁵. In addition, it is hard to believe that the C-H out-of-plane deformation mode in FTIR is sensitive to the translational motion. Furthermore, the splitting of C2 and C5 signals in CPMAS NMR spectra with heating also infers the existence of the reorientational motion. Since the C2 and C5 carbons are covalently bound, these carbons are thought of as a kind of donor-accepter pair; namely, electronic charge densities for the C2 and C5 carbons are non-equally distributed, resulting in opposite shift direction in ^{13}C chemical shielding. Taking account of both IR and NMR detectable, the most plausible reorientation is twist motion. The similar low energy excitations of twist motion were observed in structural phase transitions in oligophenylenes using Raman⁴² and NMR^{43,44}. The existence of quasi-ordered phase by twist motion was also observed in thermochromism of regiorandom P3HT⁶ and the similar polymer, poly(4-methylthiazole-2,5-diyl)³³. Since the structural modulation waves due to this twist motion show a large dispersion, from GHz to sub kHz order³³, it would be reasonable to detectable by both NMR and IR.

The temperatures where spectral and R_1 slope change occur in NMR around 323K and 333K, respectively. These are slightly higher than DSC and IR results. Generically the transition temperature detected by NMR is higher than that of DSC because NMR is sensitive to the motion with higher frequency. Therefore, NMR, DSC, and IR monitor the identical transition.

The above arguments indicate that the glass transition with respect to the thiophene twisting in the crystalline state occurs around 333K. We define the transition as a twist-glass transition.

However, the temperature dependence of the stretching parameter does not accord with the results of other glass formers. In ^2H NMR measurements, if the spin diffusion rate is sufficiently slower than the spin-lattice relaxation rate R_1 , that is, if the recoveries of magnetization directly reflect the molecular motions at that time, then the experimental data are often fitted by a single stretched-exponential function like that described in Eq. (2), from which the mean relaxation time is obtainable:

$$\hbar T_1 i = \frac{T_1}{\Gamma(x)} \quad (3)$$

where $\Gamma(x)$ is a Gamma function. For $T > T_g$, x is nearly unity because the motional correlation time is

much shorter than the spin-lattice relaxation time, which means that ergodicity is achieved. Around T_g , the value of ρ begins to decrease with decreasing temperature because of the T_1 distribution caused by the slowing of process. Then, the value of ρ increased again slightly with further cooling^{39,45,46,47}. In these cases, the single form of the spectral density function, $J(\omega)$, is used to determine T_1 because it allows the specific examination of intramolecular motions in ignorance of intermolecular interactions. In our case, because of the crystalline state of strong packing, we cannot ignore the fluctuation of intermolecular interaction, especially above the transition temperature where twist motion exists. For that reason, two kinds of spectral density functions are needed $J_{\text{intra}}(\omega)$ and $J_{\text{inter}}(\omega)$. Because two interactions, magnetic dipolar coupling and chemical shift anisotropy, should affect each $J(\omega)$ s in the specific ratio depending on the second moment of interactions, the decay curve cannot be expressed by a single stretched-exponential function, indicating that ρ cannot express the T_1 distribution directly at higher temperatures. At $T < 333\text{ K}$, where a twist motion is absent, the magnetization curve can be expressed using a single stretched-exponential function. As mentioned above, however, at least two states exist, which are attributed to 825 cm^{-1} and 810 cm^{-1} in the FTIR spectrum under the temperature region. Therefore, the value of ρ does lose the conventional meaning of the distribution parameter in the case of P3BT.

To detect more direct evidence of the twist-glass transition, we tried to perform CODEX measurements at 303K and 353K where are lower and higher than the transition temperature, respectively. Fig. 7(a) and (b) show CODEX spectra (S), reference spectra (S_0), and pure-exchange spectra ($S = S - S_0$) at 303K and 353K, respectively, with mixing time of $t_m = 120\text{ ms}$, $t_z = 0.8\text{ ms}$ and CSA recoupling time of $N_{\text{tr}} = 1\text{ ms}$. At 303K, no significant change is observed between S and S_0 , consequently S shows a weak signal; that is, sufficient motion of thiophene with detectable motional amplitude during N_{tr} ($= 1\text{ ms}$) does not occur below the twist glass transition temperature. At 353K, on the other hand, the pure-exchange spectrum shows the signal of thiophene. It indicates that thiophene main chain undergoes reorientation during the mixing time ($t_m = 120\text{ ms}$) and consequently the motion attenuates recoupling of CSA. This is a direct evidence of thiophene twisting above the twist-glass transition. Fig. 7(c) shows the normalized exchange intensity as a function of t_m . The mixing-time dependence of CODEX can be expressed as⁴⁸

$$S/S_0(t_m) = \frac{M}{M} \frac{1}{M} \frac{1}{M} \exp\left(-\frac{t_m}{\tau_c}\right); \quad (4)$$

where τ_c is the correlation time, β is the stretching parameter, and M is the number of equivalent orientational sites accessible in the motional process. Using this equation the correlation time of thiophene twist is found to be $\tau_c = 31.4\text{ ms}$ ($\beta = 31.8\text{ Hz}$) at 353K. However, it is

difficult to determine this value as a characteristic rate of thiophene twist because the twist motion shows a large dispersion because of the structural modulation waves as observed in the similar polymer P4MT³³.

D. Glassy crystal (plastic crystal) transition

We were able to detect the twist-glass transition by FTIR and ^{13}C NMR measurements. The state above the transition temperature (340 K) should be the quasi-ordered phase with a thiophene twist. As mentioned above, typical examples of the quasi-ordered phase might include liquid crystals (LCs) and the plastic crystals (PCs). If the LC and PC are cooled quickly enough, they can be frozen respectively into a glassy liquid crystalline (GLC) and a glassy crystalline (GC) state.

The appearance of LC, particularly a nematic mesophase, in regioregular P3ATs has been reported^{1,2,5}. The phenomenon has been observed just below the melting point, where π -stacking has already disappeared and only a residual order, caused by a side-by-side arrangement, remained. On the other hand, below the nematic phase, P3ATs keep the π -stacking even though the alkyl side chain is in the molten state. In this temperature range, the π -stacking is not sufficiently strong to maintain perfect planarity, but it is not too weak to show fluidity attributable to the LC state. Here, if the twist motion would be treated as a rotational freedom, we could define the P3ATs as a kind of PC. Assuming P3ATs as a class of PC, we can easily interpret the twist-glass transition around 340 K (T_{gp}) for P3BT as the transition between the glassy crystal and the plastic crystal.

The complicated wavenumber shifts in the FTIR spectra of P3BT are explained reasonably using this idea. Above T_{gp} , the dominant peak appears at 820 cm^{-1} (Fig. 2a, right), and can be assigned to the plastic crystal. Below T_{gp} , two signals are observed at 825 cm^{-1} and 810 cm^{-1} (Fig. 2a, left). The 825 cm^{-1} peak is almost constant down to 173 K, whereas 810 cm^{-1} peak increases gradually with cooling (Fig. 3). We assign the 825 cm^{-1} peak to the glassy crystal. Below T_{gp} , the intensity of the 825 cm^{-1} peak is constant, which is probably because the amount of GC cannot increase further and the twist motion of the thiophene rings is frozen. Results of temperature-dependent WAXD by Causin et al.⁵ also follow this hypothesis: at 323 K, the (010) peak, derived from the π -stacking, was not observed because the frozen thiophene rings with various twist angles smear the clear x-ray diffraction. On the contrary, at 373 K, the clear diffraction peak appears because of the averaged positional order that results from the twist motion.

Next, we specifically examine the small peak at 810 cm^{-1} of P3BT. Taking account of the absence of the twist motion below T_{gp} , which is deduced from our $T_{1\rho}$ measurements, and considerably remaining a small amount of crystal from the x-ray diffraction⁵, we can assign the

peaks at 810 cm^{-1} for P3BT and at 815 cm^{-1} for P3HT to the crystalline phase which is constituted of the planar thiophene arrangement with stronger π -stacking. Although the reasons for a gradual transition from 820 cm^{-1} to 810 cm^{-1} for P3BT and to 815 cm^{-1} for P3HT are not clear, we suggest two possible scenarios about the gradual transition. One is that the motion of the alkyl chain is a thermally activated process in the extreme narrowing regime, as shown by results of $T_{1\rho}$ measurements. The process might induce the libration-like twist motion of thiophene rings. The gradual change in the IR spectra might be attributable to gradual amplification of the libration. Another explanation is the two-dimensional melting of thiophene twist via continuous phase transition, as expressed by Kosterlitz-Thouless-Halperin-Nelson-Young (KTHNY) theory^{49,50,51,52}. We will discuss this problem in a future study.

Next, we explain why the DSC curve shows not a heat capacity jump, but an endothermic peak, if the transition is a twist-glass transition. The most reasonable explanation is that this is the effect of enthalpy relaxation of the twist-glassy state. To examine this, we tried the DSC measurement for P3BT with various aging times (Fig. 8). The growth of endothermic peaks is observed as a function of aging time. Typical heat capacity jump was not observed because the difference of heat capacity between glassy crystal and plastic crystal could be very small. Another possibility of the appearance of the endothermic peak is the order-disorder transition of thiophene ring stacking, which might be assigned to the peak shift from 810 cm^{-1} to 820 cm^{-1} in FTIR measurement. Using that possibility, we probably cannot explain the gradual change over the wide temperature range. Although the transition might be too broad and its enthalpy might be too small to estimate the heat flow of the endothermic peak, we conclude that the endothermic peak originates from the enthalpy relaxation by the glassy crystal.

E. Glassy crystals of P3AT with longer alkyl chains

Why were we able to observe the twist-glass transition only for P3BT? The most important factor is probably structural relaxation rate of the twist. The relaxation rate is determined by several factors such as the free volume, the mobility of both side chains and the main chain, the interaction between main chains, and so on. These factors are strongly dependent on the alkyl chain length.

For P3DDT, the mobility of the main chain would be restricted below 330 K because of the packing of the long side chains (Fig. 1(e)). We infer that the twist-glass transition temperature is dependent on the side chain length, as in the case of the conventional glass transition²⁹. From the analogy to the conventional glass transition of P3AT, the twist-glass transition temperature of P3DDT is presumably lower than 340 K. Such a situation would inhibit observation of the twist-glass transition because of the existence of the already crystallized alkyl chains. The

FTIR spectra of P3DDT at lower temperatures support this view (Fig. 2(c)).

On the contrary, we expect that P3HT as well can show the twist-glass transition because the side chain will take a liquid state over a wide temperature range, similarly to P3BT. We observed the peak shift at 253 K from 820 cm^{-1} to 815 cm^{-1} with cooling in the FTIR measurements (Fig. 2(b), left). Therefore, we investigated the existence of the twist-glass transition that occurs around the temperature if the cooling rate is sufficiently high to compete with the relaxation rate of twist. Unfortunately, the temperature controller in our FTIR instrument is unavailable for rapid cooling and NMR is out of the available temperature range. Therefore, we investigated the existence of the twist-glass transition in P3HT using DSC measurements (Fig. 9). We succeeded in observing the quite small endothermic peak around 250 K for the sample annealed for 12 h at 223 K after cooling from 423 K at a rate of ca. 50 K/min (Fig. 9(b)), whereas the sample without annealing showed no peak (Fig. 9(a)). Furthermore, the sample cooled from 533 K (over the melting temperature) at a rate of ca. 50 K/min shows a similar phenomenon (Fig. 9(c) and Fig. 9(d)). Interestingly, the temperature of the endothermic peak, as observed by the DSC measurements, is consistent with the temperature of the peak shift shown by FTIR measurements. Therefore, it seems that the endothermic peak observed around 250 K originates from the enthalpy relaxation of the glassy crystal, as in the case of P3BT. However, because the observed endothermic peaks are so small and close to the conventional glass transition (256 K) in the melt-quenched sample by liquid nitrogen (Fig. 9(e)), it seems to be difficult to assign the transition to the twist-glass transition.

IV. CONCLUSION

Solid-state structure and dynamics of the regioregulated HT-P3ATs, especially P3BT, were investigated using FTIR and ^{13}C NMR spectroscopies. The DSC measurements show that P3BT has an endothermic transition that occurred in the crystalline phase around 340 K. The FTIR measurements show that the shifts of absorption maximum for the out-of-plane mode of the thiophene C-H band were observed, which is consistent with DSC results. In the ^{13}C CPMAS NMR measurements, the methyl moiety shows the transition from two or more states to a unique state. Furthermore, $T_{1\rho}$ and CODEX measurements indicate that there exists a glass transition of thiophene ring twist in the crystalline phase. Its enthalpy relaxation shows an endothermic peak in DSC traces. To P3BT, we attempted to apply the idea that it is a glassy crystal-plastic crystal transition. We assigned each peak in FTIR to a specific phase. A phase diagram of P3BT is shown in Fig. 10. At temperatures higher than the melting point ($T > 540\text{ K}$), the polymer is surely an isotropic liquid assigned to 836 cm^{-1} in

the FTIR spectrum. At $340\text{ K} < T < 540\text{ K}$, mostly plastic crystal (820 cm^{-1}) exists, where the polymer undergoes the twist motion of thiophene. Below 340 K , two

states exist in which the glassy crystal (825 cm^{-1}) has thiophene rings that are frozen with various angles and crystals without twisting (810 cm^{-1}).

-
- Corresponding Author; Electronic address: nasakawa@bio.titech.ac.jp
- ¹ T. J. Prosa, M. J. Winkler, and R. D. McCullough: *Macromolecules* 29, 3654 (1996).
 - ² S. V. Meille, M. J. Winkler, and R. D. McCullough: *Macromolecules* 30, 7898 (1997).
 - ³ K. C. Park and K. Levon: *Macromolecules* 30, 3175 (1997).
 - ⁴ A. Bolognesi, W. Porzio, A. Provasoli, C. Botta, A. Comotti, P. Sozzani, and R. Simonutti: *Macromol. Chem. Phys.* 202, 2586 (2001).
 - ⁵ V. Causin, C. Marega, A. Marigo, L. Valentini, and J. M. Kenny: *Macromolecules* 38, 409 (2005).
 - ⁶ O. Inganas, W. R. Salaneck, J.-E. Oosterholm, and J. Laakso: *Synth. Met.* 22, 395 (1988).
 - ⁷ J. Corish, D. E. Feeley, D. A. Morton-Blake, F. Beniere, and M. Marchetti: *J. Phys. Chem. B* 101, 10075 (1997).
 - ⁸ K. Iwasaki, H. Fujimoto, and S. Matsuzaki: *Synth. Met.* 63, 101 (1994).
 - ⁹ Cheng Yang, Francesco Porro, and S. Holdcroft: *Macromolecules* 29, 6510 (1996).
 - ¹⁰ K. Tsuchi, M. Sorai, and S. Seki: *Bull. Chem. Soc. Jpn* 44, 1452 (1971).
 - ¹¹ G. P. Johari and J. W. Goodby: *J. Chem. Phys.* 77, 5165 (1982).
 - ¹² D. Chen and H. G. Zachmann: *Polymer* 32, 1612 (1991).
 - ¹³ O. Ahumada, T. A. Ezquerro, A. Nogales, F. J. Balta-Calleja, and H. G. Zachmann: *Macromolecules* 29, 5002 (1996).
 - ¹⁴ A. del Campo, A. Bello, and E. Perez: *Macromol. Chem. Phys.* 203, 2508 (2002).
 - ¹⁵ S. H. Chen, H. M. Phillip Chen, Y. Geng, S. D. Jacobs, K. L. Marchell, and T. N. Blanton: *Adv. Mater.* 15, 1061 (2003).
 - ¹⁶ M. Tokita, S. Funaoka, and J. Watanabe: *Macromolecules* 37, 9916 (2004).
 - ¹⁷ K. Adachi, H. Suga, and S. Seki: *Bull. Chem. Soc. Jpn* 41, 1073 (1968).
 - ¹⁸ R. Tycko: *Solid State NMR* 3, 303 (1994).
 - ¹⁹ T. Pietrass, R. Seydoux, R. E. Roth, H. Eckert, and A. Pines: *Solid State NMR* 8, 265 (1997).
 - ²⁰ J. P. Amoureux, R. Decressain, M. Sahour, and E. Cochon: *J. Phys. II France* 2, 249 (1998).
 - ²¹ R. Decressain, L. Carpentier, and M. Descamps: *J. Chem. Phys.* 122, 034507 (2005).
 - ²² (a) T.-A. Chen and R. D. Rieke: *J. Am. Chem. Soc.* 114, 10087 (1992). (b) T.-A. Chen and R. D. Rieke: *Synth. Met.* 60, 175 (1993). (c) X. Wu, T.-A. Chen, and R. D. Rieke: *Macromolecules* 28, 2101 (1995). (d) T.-A. Chen, X. Wu, and R. D. Rieke: *J. Am. Chem. Soc.* 117, 223 (1995).
 - ²³ E. O. Stejskal, J. Schaefer, and J. S. Waugh: *J. Magn. Reson.* 28, 105 (1977).
 - ²⁴ E. R. deAzevedo, W.-G. Hu, T. J. Bonagamba, and K. Schmidt-Rohr: *J. Am. Chem. Soc.* 121, 8411 (1999).
 - ²⁵ D. A. Torchia: *J. Magn. Reson.* 30, 613 (1978).
 - ²⁶ D. Ditchfield: *Mol. Phys.* 27, 789 (1974).
 - ²⁷ K. W. Olinsky, J. F. Hinton, and P. Pulay: *J. Am. Chem. Soc.* 112, 8251 (1990).
 - ²⁸ Gaussian 98, Revision A.7, M. J. Frisch, G. W. Trucks, H. B. Schlegel, G. E. Scuseria, M. A. Robb, J. R. Cheeseman, V. G. Zakrzewski, J. A. Montgomery, Jr., R. E. Stratmann, J. C. Burant, S. Dapprich, J. M. Millam, A. D. Daniels, K. N. Kudin, M. C. Strain, O. Farkas, J. Tomasi, V. Barone, M. Cossi, R. Cammi, B. Mennucci, C. Pomelli, C. Adamo, S. Cliford, J. Ochterski, G. A. Petersson, P. Y. Ayala, Q. Cui, K. Morokuma, D. K. Malick, A. D. Rabuck, K. Raghavachari, J. B. Foresman, J. Cioslowski, J. V. Ortiz, A. G. Baboul, B. B. Stefanov, G. Liu, A. Liashenko, P. Piskorz, I. Komaromi, R. Gomperts, R. L. Martin, D. J. Fox, T. Keith, M. A. Al-Laham, C. Y. Peng, A. Nanayakkara, C. Gonzalez, M. Challacombe, P. M. W. Gill, B. Johnson, W. Chen, M. W. Wong, J. L. Andres, C. Gonzalez, M. Head-Gordon, E. S. Replogle, and J. A. Pople, (Gaussian, Inc., Pittsburgh PA, 1998).
 - ²⁹ S.-A. Cheng and J.-M. Ni: *Macromolecules* 25, 6081 (1992).
 - ³⁰ M. Letz, R. Schilling, and A. Latz: *Phys. Rev. E*, 62, 5173 (2000).
 - ³¹ G. Zerbi, B. Chierichetti, and O. Inganas: *J. Chem. Phys.* 94, 4646 (1991).
 - ³² G. Barbarella, D. Casarini, M. Zambianchi, L. Favaretto, and S. Rossini: *Adv. Mater.* 8, 69 (1996).
 - ³³ S. Mori, Y. Inoue, T. Yamamoto, and N. Asakawa: *Phys. Rev. B* 71, 054205 (2005).
 - ³⁴ N. Bloembergen, E. M. Purcell, and R. V. Pound: *Phys. Rev.* 73, 679 (1948).
 - ³⁵ F. Kohlrausch: *Prog. Ann. Phys.*, 119, 352 (1863); G. Williams and D. C. Watts: *Trans. Faraday Soc.* 66, 80 (1970).
 - ³⁶ W. Schnauss, F. Fjara, K. Hartmann, and H. Sillescu: *Chem. Phys. Lett.* 166, 1378 (1992).
 - ³⁷ R. Bohmer, G. Diezmann, G. Hinze, and E. Rossler: *Prog. NMR Spectrosc.* 39, 191 (2001).
 - ³⁸ E. Rossler, U. Warschewske, P. Eiermann, A. P. Sokolov, and D. Quirann: *J. Non-Cryst. Solids* 172-174, 113 (1994).
 - ³⁹ A. Do, G. Hinze, G. Diezmann, and R. Bohmer: *Acta Polymer* 49, 56 (1998).
 - ⁴⁰ G. P. Johari and M. Goldstein: *J. Chem. Phys.* 53, 2372 (1970).
 - ⁴¹ A. Abragam: *Principles of Nuclear Magnetism* (Clarendon Press, Oxford, 1961).
 - ⁴² S. Guha, W. Graupner, R. Resel, M. Chandrasekhar, H. R. Chandrasekhar, R. Glaser, and G. Leising: *Phys. Rev. Lett.* 82, 3625 (1999).
 - ⁴³ K. Kohda, N. Nakamura, and H. Chihira: *J. Phys. Soc. Jpn.* 51, 3936 (1982).
 - ⁴⁴ S.-B. Liu and M. S. Conradi: *Phys. Rev. Lett.* 54, 1287 (1985).
 - ⁴⁵ G. Hinze and H. Sillescu: *J. Chem. Phys.* 104, 314 (1996).
 - ⁴⁶ A. Do, G. Hinze, R. Bohmer, H. Sillescu, H. Kolshorn, M. Vogel, and H. Zimmermann: *J. Chem. Phys.* 112, 9455 (2000).

- ⁴⁷ R. Bohmer, G. Hinze, T. Jorg, F. Qi, and H. Sillescu: Prog. J. Phys. Condens. Matter. 12, A 383 (2000).
- ⁴⁸ E. R. deAzevedo, W. -G. Hu, T. J. Bonagamba, and K. Schmidt-Rohr: J. Chem. Phys. 112, 8988 (2000).
- ⁴⁹ J. M. Kosterlitz and D. J. Thouless: J. Phys. C: Solid State Phys. 6, 1181 (1973).
- ⁵⁰ B. I. Halperin and D. R. Nelson: Phys. Rev. Lett 41, 121 (1978).
- ⁵¹ D. R. Nelson and B. I. Halperin: Phys. Rev. B 19, 2457 (1979).
- ⁵² A. P. Young: Phys. Rev. B 19, 1855 (1979).

TABLE I: Observed isotropic determined by ^{13}C CPMAS NMR (units in parts per million from tetramethylsilane)

T (K)	alkyl chain				thiophene ring			
	C2 ⁰	C1 ⁰	C3 ⁰	C4 ⁰	C3	C2	C5	C4
303	33.3	30.5	23.7	16.1, 14.8	136.4	132.6	131.4	126.3
313	33.2	30.4	23.6	15.9, 14.7	136.3	132.5	131.2	126.1
323	33.3	30.4	23.6	15.8, 14.6	136.2	132.7	131.1	126.1
333	33.1	30.3	23.6	15.7, 14.6	136.2	132.8	131.1	126.0
343	33.1	30.2	23.5	14.6	136.0	132.7	130.9	125.9
353	33.2	30.3	23.7	14.6	136.1	132.8	131.0	126.1
373	33.2	30.3	23.7	14.6	136.1	132.9	131.1	126.2

TABLE II: Principal components of nuclear shielding for ring carbons in HT-tri(3METH) calculated by the GIAO-CHF method with 6-31G (d) (units in parts per million).

nucleus	iso	11	22	33
C2	73.49	-5.40	73.94	151.94
C3	72.02	-0.21	52.31	163.95
C4	79.72	6.38	87.31	145.46
C5	62.10	-24.30	57.70	152.90

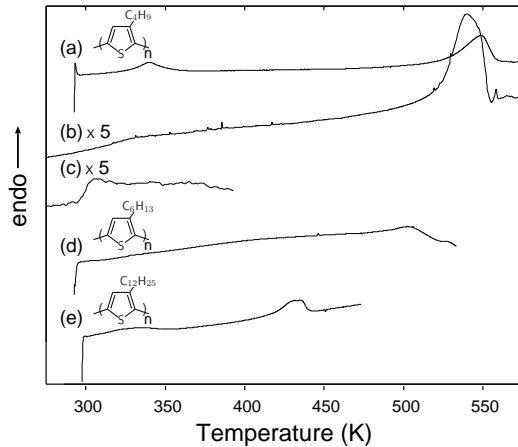


FIG. 1: DSC charts for powder samples of the first heating scan for P3BT (a), P3HT (d), and P3DDT (e), and the second heating scan for P3BT (b), and (c). The heating rate was 10 K/m in. After the first heating scan, the P3BT were cooled at ca. 50 K/m in (b) or quenched by liquid nitrogen (c) and the second scan was run.

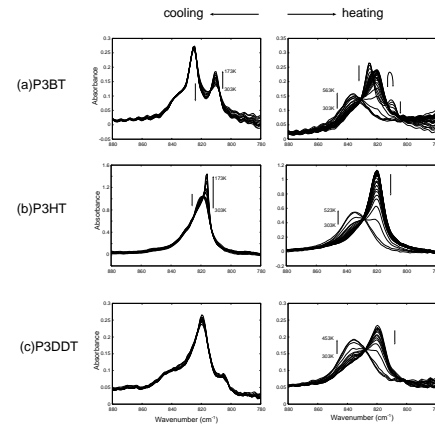


FIG. 2: Temperature dependence of infrared absorption spectra of thin films for P3BT (a), P3HT (b), and P3DDT (c) thin films. Only the C-H out-of-plane deformation band region is shown.

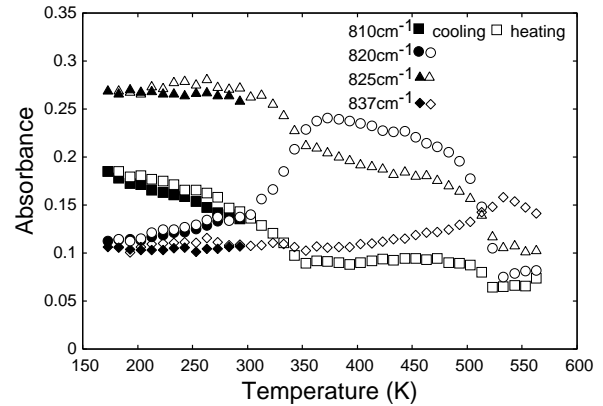


FIG. 3: Change in the absorption of the C-H out-of-plane deformation band for P3BT. At first, the sample was cooled from 303 K to 173 K, and after 3 min in storage heated from 173 K to 573 K with the rate of 10 K/m in.

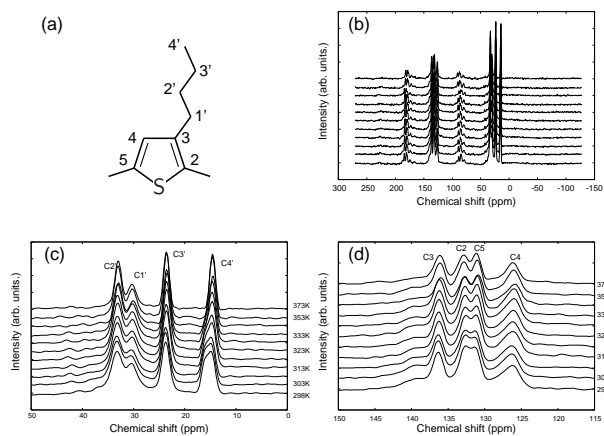


FIG . 4: Temperature variation of ^{13}C CPMAS NMR spectra for P3BT. The chemical structure (a), the whole range of spectra (b), and the extended spectra for the alkyl carbons (c), and the thiophene ring (d) are shown.

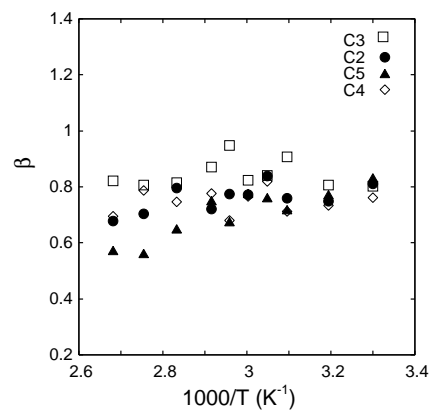


FIG . 6: Temperature variation of the stretching parameter β .

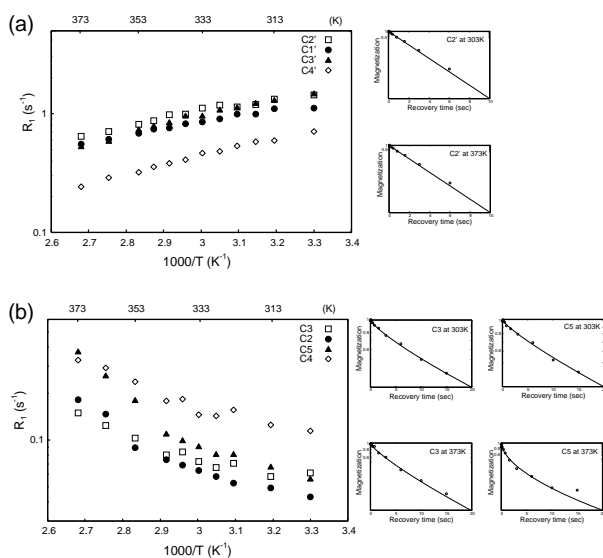


FIG . 5: Plots of ^{13}C spin-lattice relaxation rate R_1 as a function of $1000/T$ for P3BT; the alkyl side chain (a) and the main chain (b). Typical decay curves are also shown for the butyl $\text{C}2'$ carbon, and for the thiophene $\text{C}3$ and $\text{C}5$ carbons at 303 K and 373 K (insets).

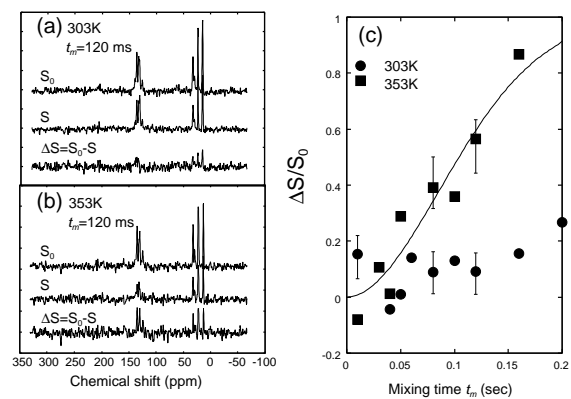


FIG . 7: A pure-exchange spectrum (S) from a CODEX measurement (S) and a reference spectrum without exchange (S_0) at 303K (a) and 353K (b). S was generated by subtraction of S from S_0 . S/S_0 of thiophene twisting at 303 K and 353 K were plotted as a function of t_m (c).

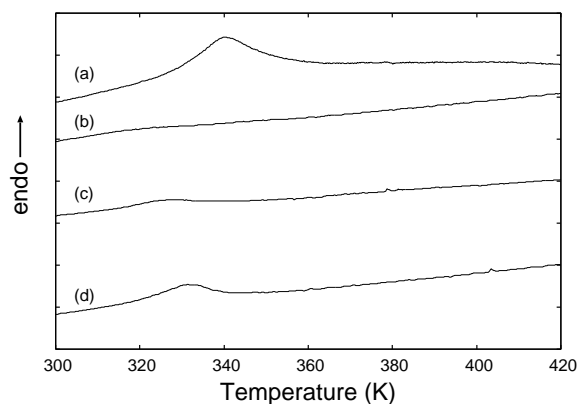


FIG . 8: DSC heating thermograms of the original sample (a) and 1 h storage at 298 K (b), 24 h (c), and 4 weeks (d) for P3BT after annealing at 423 K for 3 min and cooling at the rate of 10 K/min.

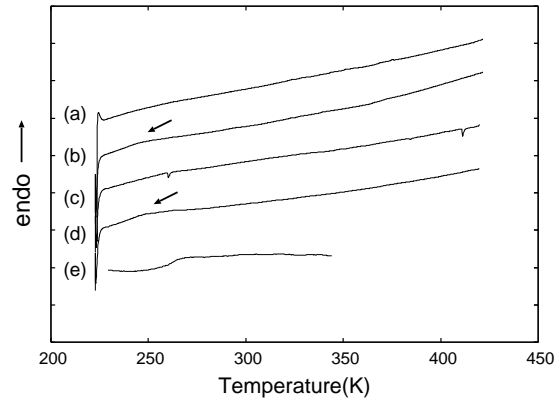


FIG. 9: DSC heating thermograms for the P3HT sample stored at 223 K for 1 min in (a) and for 12 hours (b) after cooling from 423 K at a rate of ca. 50 K/min, for 1 min in (c) and 12 h storage (d) after cooling from 533 K at a rate of ca. 50 K/min, and for the quenched sample by liquid nitrogen from 533 K (e).

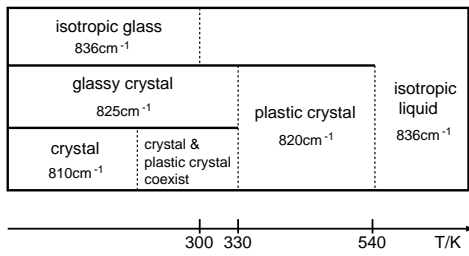


FIG. 10: A proposed phase diagram of P3BT. The IR absorption bands for the C-H bond out-of-plane deformation are also shown.

SUPPLEMENTARY MATERIALS

V. EXPERIMENTS

We carried out variable temperature proton transverse relaxation time (T_{2H}) measurements, at 270 MHz for 1H with a home-built micro-coil probe. The experimental conditions was set up with 90 pulse length of 2.3 μ s for T_{2H} measurements. We used two-pulse Hahn echo method¹ for T_{2H} measurements.

VI. RESULTS AND DISCUSSION

The 1H NMR spin echo spectra with echo time of 5 s at 303K, 333K, and 363K were shown in Fig 1(a). We should pay attention to the broader component of spectra for investigating the C4 carbon because the main chain must be more rigid than the alkyl side chain. While the number of protons in the thiophene monomer unit is unity, nine protons are in alkyl chain. In the light of this, the broader component of the spectra originate from not only the thiophene proton but also the moieties of the alkyl chain because the relative intensity of the broader component is much larger than 0.1. Generically, the TPHE decay in rigid lattice can be fitted with

$$M_z(t) = M(0) \exp\left(-\frac{t}{T_2}\right) \exp\left[-\left(\frac{t}{T_G}\right)^2\right]; \quad (5)$$

where $M(0)$, T_2 , T_G , and t denote the initial transverse magnetization, the transverse relaxation time, the characteristic decay time of the Gaussian component, and time, respectively. In our results, however, we could not

estimate the amount of the Gaussian component because the signal from the thiophene proton was overwhelmed by signals from the alkyl protons. There is yet another possible case where at room temperature ($T < T_{gp}$) the thiophene proton is decoupled with the surrounding protons due to rapid molecular motion of alkyl chains. In this case, the signal of the thiophene proton should have a Lorentzian shape. In any cases, the decay of broader signal must be originated from multiple components because of signals derived from both thiophene and alkyl protons. Therefore, we fitted the decay with a sum of two Lorentzian curves, given by

$$M_z(t) = M_f(0) \exp\left(-\frac{t}{T_{2f}}\right) + M_s(0) \exp\left(-\frac{t}{T_{2s}}\right); \quad (6)$$

where T_{2f} and T_{2s} denote lifetimes for faster and slower decays, and $M_f(0)$ and $M_s(0)$ are the respective intensity at $t=0$. Since the proton in thiophene must be included in faster decay component, we carried out the Arrhenius plot of spin-spin relaxation rate ($R_2 = T_2^{-1}$) of the broader signal (in Fig.1(b), typical decay curves at 303K and 363K are also shown in insets). The value of R_2 decreases with heating, although no sudden change was observed with respect to the transition around 340K. Therefore, the motional narrowing of the local dipolar field occurs over the measuring temperature range. However, in ^{13}C CPMAS spectra, dynamic averaging of chemical shift distribution due to the twist motion possibly causes the narrowing of the C4 signal. The latter possibility cannot be ruled out only from the T_{2H} measurements. Conclusively, we could not identify the reason for the signal narrowing of the C4 carbon of thiophene in association with temperature elevation.

Corresponding Author; Electronic address: nasakawa@bio.titech.ac.jp

¹ E.L.Hahn: Phys. Rev. 80, 580 (1950).

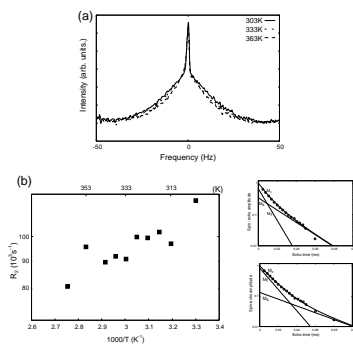


FIG. 11: ^1H two-pulse Hahn echo spectra with echo time of 5 s at 303K, 333K, and 363K (a). Plots of ^1H spin-spin relaxation rate R_2 of the broader component as a function of inverse temperature, $1000/T$ (b). Typical decay curves at 303K and 363K are also shown in insets. All decay curves were normalized so that the value at zero time equals unity.